*Research Article*

MOLECULAR PAIN

Molecular Pain
Volume 12: 1–16

DOI: 10.1177/1744806916653969
mpx.sagepub.com
SAGE

# Functional inhibition of chemokine receptor CCR2 by dicer-substrate-siRNA prevents pain development

**Valérie Bégin-Lavallée, MSc[1,*], Élora Midavaine, BS[1,*], Marc-André Dansereau, PhD[1], Pascal Tétreault, PhD[1], Jean-Michel Longpré, PhD[1], Ashley M Jacobi, BS[2], Scott D Rose, PhD[2], Mark A Behlke, MD, PhD[2], Nicolas Beaudet, PhD[3] and Philippe Sarret, PhD[1]**

## Abstract

**Background:** Accumulating evidence suggests that the C-C chemokine ligand 2 (CCL2, or monocyte chemoattractant protein 1) acts as a neuromodulator in the central nervous system through its binding to the C-C chemokine receptor 2 (CCR2). Notably, it is well established that the CCL2/CCR2 axis plays a key role in neuron-glia communication as well as in spinal nociceptive transmission. Gene silencing through RNA interference has recently emerged as a promising avenue in research and drug development, including therapeutic management of chronic pain. In the present study, we used 27-mer Dicer-substrate small interfering RNA (DsiRNA) targeting CCR2 and assessed their ability to reverse the nociceptive behaviors induced by spinal CCL2 injection or following intraplantar injection of complete Freund's adjuvant.

**Results:** To this end, we first developed high-potency DsiRNAs designed to target different sequences distributed across the rat CCR2 (rCCR2) messenger RNA. For optimization, methyl groups were added to the two most potent DsiRNA candidates (Evader and M7 2′-O-methyl modified duplexes) in order to improve in vivo duplex stability and to reduce potential immunostimulatory activity. Our results demonstrated that all modified candidates formulated with the cell-penetrating peptide reagent Transductin showed strong RNAi activity following intrathecal delivery, exhibiting >50% rCCR2 knockdown in lumbar dorsal root ganglia. Accordingly, we found that these DsiRNA duplexes were able to reduce spinal microglia activation and were effective at blocking CCL2-induced mechanical hypersensitivity. Along with similar reductions of rCCR2 messenger RNA, both sequences and methylation patterns were similarly effective in inhibiting the CCL2 nociceptive action for the whole seven days testing period, compared to mismatch DsiRNA. DsiRNAs against CCR2 also reversed the hypernociceptive responses observed in the complete Freund's adjuvant-induced inflammatory chronic pain model.

**Conclusion:** Altogether, these results validate CCR2 as a an appropriate molecular target for pain control and demonstrate that RNAi-based gene therapy represent an highly specific alternative to classical pharmacological approaches to treat central pathologies such as chronic pain.

## Keywords

DsiRNA, gene silencing, chemokines, MCP-1, Transductin, mechanical allodynia, CCL2

Date received: 23 December 2015; revised: 10 May 2016; accepted: 16 May 2016

[1]Department of Pharmacology and Physiology, Institut de Pharmacologie de Sherbrooke, Faculty of Medicine and Health Sciences, Université de Sherbrooke, Sherbrooke, QC, Canada
[2]Integrated DNA Technologies Inc, Coralville, IA, USA
[3]Department of Anesthesiology, Faculty of Medicine and Health Sciences, Université de Sherbrooke, Sherbrooke, QC, Canada

*These authors contributed equally

**Corresponding author:**
Philippe Sarret, Department of Pharmacology and Physiology, Faculty of Medicine and Health Sciences, Université de Sherbrooke, 3001, 12th Avenue North, Sherbrooke, QC, Canada.
Email: Philippe.Sarret@USherbrooke.ca

## Background

Chemokines are chemotactic cytokines originally known for their role in inflammatory responses and leukocyte attraction to injured sites in the periphery.[1,2] In recent years, chemokines were found to be constitutively expressed in the central nervous system (CNS) and to act as neurotransmitters and neuroimmune regulators.[3] As such, some chemokines modulate nociceptive processing by directly increasing sensory neuron activity and by inducing glial cell activation.[4,5] Therefore, chemokines appear to play a key role in the initiation and maintenance of persistent pain states.[6–8]

Among chemokines, C-C chemokine ligand 2 (CCL2), formerly known as monocyte chemoattractant protein-1 (MCP-1), is involved in spinal nociceptive processing through activation of its cognate receptor C-C chemokine receptor 2 (CCR2).[9] Indeed, a single intrathecal (i.t.) injection of exogenous CCL2 provokes rapid and sustained mechanical allodynia in healthy rats.[10–12] Accordingly, CCR2 receptor antagonists successfully inhibit nociceptive signaling in acute, inflammatory, and neuropathic pain in animal models.[11,13–18] These behavioral observations are further supported by genetic evidence as CCL2 overexpressing mice show greater nociceptive responses in both thermal and chemical stimulus modalities.[19] In addition, CCR2-deficient mice exhibit decreased nociceptive behaviors to formalin-induced prolonged noxious stimulation, fail to develop neuropathic pain, and do not display movement-evoked pain behaviors in osteoarthritis.[20,21]

Recent studies highlighted the chemokine system as a promising new therapeutic target for pain management.[22] However, the redundancy and promiscuity of the chemokine world pose a serious challenge for chemokine receptor-targeted drug development.[23] Indeed, chemokines tend to bind to multiple chemokine receptors expressed on a variety of cell types and, in turn, several chemokine receptors often bind multiple chemokines.[1] Given their large size, endogenous chemokines predominantly interact with extracellular domains of their receptor, while small molecules often act more deeply in an allosteric mode to stabilize the targeted receptor in a particular conformation.[24–26] It makes specific antagonists hard to design and may explain in part the failure currently faced in the development of antagonists targeting chemokine receptors.[27,26]

In recent years, gene silencing through RNA interference (RNAi) became a promising tool in research and drug development.[28–32] Its broad applicability, high efficiency, and specificity distinguish this technology from traditional drugs and may be useful to target complex systems, such as the chemokine network. In RNAi technology, small interfering RNAs (siRNA) are actually the most employed research tools. They are double-stranded synthetic 21-mer RNA duplexes developed to mimic Dicer's processing of long RNA substrates into small interfering fragments. Following their entry into the cell, exogenous siRNAs induce gene silencing by endogenous RNAi pathways. They are incorporated into the RNA-induced silencing complex (RISC) and induce the degradation of specific messenger RNAs (mRNA). However, the main hurdles with siRNA-based therapies are induction of off-target effects (OTEs), efficient delivery to the targeted tissues, and the triggering of innate immune responses via Toll-like receptors (TLR).[33–35] Dicer-substrate-siRNAs (DsiRNA), which consist of 27-mer double-stranded RNA (dsRNA) with 2-nt 3′ overhangs,[36] represent an alternative approach to minimize such side effects. DsiRNA length mimics Dicer substrates allowing them to pass from the Dicer enzyme to RISC complex with strand-specific orientation.[37,38] Compared to standard 21-mer siRNA, the preassociation with Dicer facilitates the incorporation of DsiRNA into the RISC complex and the loading of the guide strand into the argonaute protein Ago2.[39] In fact, the 27-mer DsiRNA were found to be up to 10-fold more potent in silencing the targeted gene than shorter 21-mers.[40–42] Moreover, the in vivo use of DsiRNAs injected directly into the CNS showed good efficiency with long-lasting behavioral actions.[43]

The aim of the present study was thus to investigate the potential use of DsiRNAs to silence CCR2 gene expression and assess their ability to reverse the nociceptive behaviors induced by spinal CCL2 injection or by intraplantar injection of complete Freund's adjuvant. To this purpose, a series of DsiRNA candidates targeting CCR2 were designed and validated both in vitro and in vivo.

## Methods

### *DsiRNAs design*

All chemical DsiRNAs described in this study were synthesized by IDT (Integrated DNA Technologies, Coralville, IA). The identity of each duplex was verified by electrospray-ionization mass spectrometry (ESI-MS) and was within $\pm 0.02\%$ predicted mass. Purification was performed by high-performance liquid chromatography and compounds were $> 90\%$ pure. Finally, the duplexes were prepared as sodium salts and differ by specific recognition sites on rat CCR2 (rCCR2) mRNA and chemical modifications. Table 1 shows the sequence of each DsiRNA candidate, while Table 2 indicates the number and positioning of methyl groups in the modified leads.

### *In vitro DsiRNA transfection and quantitative real-time PCR*

HEK293 cells stably expressing the rat CCR2 receptor (kindly provided by Pfizer, UK) were cultured ($1.3 \times 10^5$ cells) in 48-well culture plates with F12 medium supplemented with 10% fetal bovine serum, 1% penicillin/streptomycin, 0.1 mM nonessential amino acids,

**Table 1.** Nucleotide sequences of sense and antisense strands of anti-rCCR2 DsiRNA.

| Anti-rCCR2 DsiRNA | Sequences |
|---|---|
| Rn CCR2-1 | 5 pCCAGGAAUCAUAUUUACUAAAUCtg 3′ |
| | 3′AUGGUCCUUAGUAUAAAUGAUUUAGAC 5′ |
| Rn CCR2-2 | 5′ pGGAAGAAUUUCCAAACAAUAAUGag 3′ |
| | 3′GACCUUCUUAAAGGUUUGUUAUUACUC 5′ |
| Rn CCR2-3 | 5′ pACUCCAUACAAUAUUGUUCUCUUcc 3′ |
| | 3′CCUGAGGUAUGUUAUAACAAGAGAAGG 5′ |
| Rn CCR2-4 | 5′ pGCAAAUUGGAGCUUGGAUCCUGCcc 3′ |
| | 3′UUCGUUUAACCUCGAACCUAGGACGGG 5′ |
| Rn CCR2-5 | 5′ pGGAGACAGCAGACCGAGUGAGCUca 3′ |
| | 3′UCCCUCUGUCGUCUGGCUCACUCGAGU 5′ |
| Rn CCR2-6 | 5′ pUGCGUUAAUCCUAUCAUUUAUGCct 3′ |
| | 3′CGACGCAAUUAGGAUAGUAAAUACGGA 5′ |
| Rn CCR2-7 | 5′ pCCAUGGCAUACUAUCAACAUCUCat 3′ |
| | 3′UAGGUACCGUAUGAUAGUUGUAGAGUA 5′ |
| Rn CCR2-8 | 5′ pACCGUAUGACUAUGAUGAUGGUGaa 3′ |
| | 3′UGUGGCAUACUGAUACUACUACCACUU 5′ |
| Rn CCR2-9 | 5′ pGAAGAUGAUCAGCAUACUUGUGGcc 3′ |
| | 3′UUCUUCUACUAGUCGUAUGAACACCGG 5′ |
| Rn CCR2-10 | 5′ pUGCACUUAGACCAGGCCAUGCAGgt 3′ |
| | 3′GUACGUGAAUCUGGUCCGGUACGUCCA 5′ |

Upper case letter represent RNA bases while lower case letters correspond to DNA bases. p represents 5′-phosphate.

**Table 2.** Modifications on the anti-rCCR2 DsiRNA leads.

| Anti-rCCR2 DsiRNAs | Sequences |
|---|---|
| Rn NC1M7 | 5′ pGGCGCGUAUAGUCGCGCGUAUAGtc |
| | 3′ **CUC**C**G**C**G**CAUAUCA**G**C**G**CGCAUAUCAGp |
| Rn CCR2-5Evader | 5′ pGGAGACAGCAGACCGAGUGAGCUca |
| | 3′ **UCC**C**U**C**U**G**U**C**G**U**C**U**G**G**C**UCACUCGAGUp |
| Rn CCR2-6Evader | 5′ pUGCGUUAAUCCUAUCAUUUAUGCct |
| | 3′ **CGA**C**G**C**A**A**U**U**A**G**G**A**U**A**G**UAAAUACGGAp |
| Rn CCR2-5M7 | 5′ pGGAGACAGCAGACCGAGUGAGCUca |
| | 3′ **UCC**C**U**C**U**GUCGUCU**G**G**C**UCACUCGAGUp |
| Rn CCR2-6M7 | 5′ pUGCGUUAAUCCUAUCAUUUAUGCct |
| | 3′ **CGA**C**G**C**A**AUUAGGA**U**A**G**UAAAUACGGAp |

Underlined bold nucleotides correspond to methylation sites. Upper case letters represent RNA bases while lower case letters correspond to DNA bases. p represents 5′-phosphate.

0.75 mg/ml G418, and 1 μg/ml puromycin. When 40–50% confluence was reached, three different wells were independently transfected with anti-rCCR2 DsiRNA or the mismatch control (NC1M7) at 0.1 nM, 1 nM, or 10 nM and formulated with 10 nM of 1 μL of RNAiMAX (Invitrogen, Carlsbad, CA) 20 min before transfection. Total RNA was extracted 24 h after transfection using a SV96 total RNA isolation system (Promega, Madison, WI). RNA quality was verified using a Bioanalyzer 2100 (Agilent, Palo Alto, CA). Reverse transcription was performed using 150 ng of total RNA and 20 U of SuperScript II Reverse Transcriptase (Invitrogen, Carlsbad, CA) with both random hexamer and oligo-dT primers. Real-time PCR was performed in triplicate for each cDNA sample using Light Cycler 480 probe master mix using the unit Light Cycler 480 (Roche Applied Science, Indianapolis, IN). rCCR2 expression levels were analyzed by absolute expression and normalized against the internal control RLPO reporter gene. HPRT gene was used as a positive control. Normalized mRNA expression level of rCCR2 obtained by the mismatch negative control was set at 100%. Primers sequences are presented in Table 3.

## *Animals*

Adult male Sprague-Dawley rats (200–225 g, Charles River Laboratories, St-Constant, Québec, Canada) were housed three per cage on a 12-h light/dark cycle. Food and water were available ad libitum. Behavioral experiments were performed between 8 a.m. and 4 p.m. The experimental procedures performed on animals were approved by the Ethical Committee for Animal Care and Experimentation of the Université de Sherbrooke and carried out according to the regulations of Canadian Council on Animal Care. Rats were acclimatized four days to the animal facility and three days to the devices prior to behavioral studies.

## *Intrathecal administration of DsiRNAs/Drug delivery*

DisRNAs were formulated with a delivery reagent called Transductin which contains a Peptide Transduction Domain (PTD) linked to a dsRNA binding protein. Transductin has been shown to facilitate cell penetration through the process of macropinocytosis.[44] Thus, anti-rCCR2 DsiRNAs or mismatch controls suspended in sterile saline were mixed with the peptide-based transfection reagent Transductin (Integrated DNA Technologies) at a ratio of 1:15. DsiRNAs were kept on ice 40 min before i.t. injection. Under light anesthesia (2% isoflurane), rats received two injections of DsiRNAs (5 μg each in 25 μL) or saline intrathecally between vertebrae L5 and L6 ($t = 0$ h, $t = 24$ h). Subsequently, rats received a third i.t. injection ($t = 48$ h) of saline or CCL2 (1 μg) (Peprotech Inc, Rocky Hill, NJ).

## *Behavioral testing*

Mechanical allodynia was assessed using an automatic von Frey dynamic plantar aesthesiometer (Ugo Basile, Stoelting, IL). Rats were placed in individual elevated Plexiglass boxes with a wire mesh floor to which they were habituated for three consecutive days. The plantar surface of each hindpaw was stimulated by a single

**Table 3.** Primer sequences used for quantitative real-time RT-PCR analysis.

| Primer name | Forward sequence | Reverse sequence |
|---|---|---|
| HsRLPO | | |
| - Hs RLPO | AGACTGGAGACAAAGTGGGA | CAGACAGACACTGGCAACA |
| - Hs RLPO FAM | FAM/AAGCCACGCTGCTGAACATGCTCAA/3IABkFQ | |
| - Hs RLPO MAX | MAXN/AAGCCACGCTGCTGAACATGCTCAA/3IABkFQ | |
| HsHPRT | | |
| - Hs HPRT | GACTTTGCTTTCCTTGGTCAGGCA | GGCTTATATCCAACACTTCGTGGG |
| - Hs HPRT FAM | FAM/ATGGTCAAGGTCGCAAGCTTGCTGGT/3IABkFQ | |
| - Hs HPRT MAX | MAXN/ATGGTCAAGGTCGCAAGCTTGCTGGT/3IABkFQ | |
| RnHPRT | | |
| - Rn HPRT | CGAGATGTCATGAAGGAGATGG | GTAATCCAGCAGGTCAGCAAAG |
| - Rn HPRT FAM | FAM/ATCACATTGTGGCCCTCTGTGTGCTGAA/3IABkFQ | |
| - Rn HPRT MAX | MAXN/ATCACATTGTGGCCCTCTGTGTGCTGAA/3IABkFQ | |
| RnOdc | | |
| - Rn Odc | TGACATTGGTGGTGGCTTTC | GCTCAGCTATGATTCTCACTCC |
| - Rn Odc FAM | FAM/ACCAGTGTAATCAACCCAGCTCTGGACA/3IABLFQ | |
| - Rn Odc MAX | MAXN/ACCAGTGTAATCAACCCAGCTCTGGACA/3IABkFQ | |
| RnCCR2 | | |
| - Rn CCR2 | GCTGTGAGGCTCATCTTT | CCACACAGTTACTCATTCCC |
| - Rn CCR2 FAM | FAM/TTCTCTTCCTGACCACCTTCCAGGAA/3IABLFQ | |
| - Rn CCR2 MAX | MAXN/TTCTCTTCCTGACCACCTTCCAGGAA/3IABkFQ | |
| RnCCL2 | | |
| - Rn CCL2 | CTTCTGGGCCTGTTGTTC | TCTCTCTCTTGAGCTTGGT |
| - Rn CCL2 FAM | FAM/TGTCTCAGCCAGATGCAGTTAATGCC/3IABLFQ | |
| - Rn CCL2 MAX | MAXN/TGTCTCAGCCAGATGCAGTTAATGCC/3IABkFQ | |

filament (0.5 mm in diameter) of the electronic von Frey device. The force applied under the hindpaw increased from 1 to 50 g over a 20 s period (3.33 g/s) and automatically stopped by paw withdrawal response. Four successive stimuli were alternatively applied to both hindpaws at 20 s intervals. Prebaseline test were conducted prior to DsiRNA injection to ensure that duplexes do not alter mechanical sensitivity. Baseline thresholds were measured prior to i.t. administration of either saline (vehicle) or 1 μg CCL2. Rats were tested 1 h, 2 h, 4 h, and daily for seven consecutive days following i.t. injection.

## *In vivo detection of fluorescent DsiRNAs*

Sprague-Dawley rats received two i.t. injections ($t = 0$ h and $t = 24$ h) of NC1 Texas-Red-labeled or NC1 unlabeled DsiRNAs (5 μg) following the same preparation as described above. For tissue harvest, animals were deeply anesthetized with 5% isoflurane and a transaortic perfusion was performed with a freshly prepared 4% paraformaldehyde solution in 0.1 mol/L phosphate buffer solution (PBS), pH 7.4. Dorsal root ganglion (DRGs) of L4 to L6 lumbar vertebrae were rapidly isolated, postfixed for 30 min in 4% paraformaldehyde, and then cryoprotected in 30% sucrose PBS. Tissues were then sectioned at 20 μm with a cryostat (Leica CM1850). The sections were mounted on SuperFost Plus slides (VWR, Ontario, Canada) and coverslipped with Aqua-Poly/Mount (Polysciences, Nile, IL). The labeled structures were analyzed by confocal microscopy using the Olympus fluoview FV1000 laser-scanning microscope equipped with an Olympus BX61 automated research microscope.

## *Ex vivo molecular analysis*

Rats were anesthetized and intra-aortically perfused with 40 ml of saline. DRGs from L4 to L6 lumbar vertebrae were harvested 24 h after the last injection of DsiRNAs. Tissues were rapidly snap-frozen and then kept at −80°C. Total RNA was extracted from L4 to L6 DRG tissues with Trizol according to manufacturer's protocol (Invitrogen). Extracted RNA was pretreated with DNAse before reverse transcription reaction. Quantitative PCR was performed on an Applied Biosystem 7900HT Fast Real-Time PCR System. Data were collected and analyzed using ABI 7900HT SDS version 2.4 software. rCCR2 and rCCL2 gene expression

levels were analyzed by relative quantification using Odc and HPRT as reporter genes. Primers sequences are presented in Table 3.

### Glial cell activation

Under light anesthesia (isoflurane 2%), rats received two anti-rCCR2 DsiRNA (CCR2-6M7) or mismatch control injections ($t = 0$ h, $t = 24$ h) and a single CCL2 or saline injection ($t = 48$ h) as described above. Saline controls received three i.t. saline injections following the same injection protocol as the DsiRNA-treated animals ($t = 0$ h, $t = 24$ h, and $t = 48$ h). Twenty-four hours following the last injection, rats were deeply anesthetized with 5% isoflurane and intra-aortically perfused with 500 ml of freshly prepared 4% paraformaldehyde solution in 0.1 mol/L PBS, pH 7.4. L3 to L6 spinal cord sections were dissected and postfixed overnight in 4% paraformaldehyde at 4°C and then cryoprotected in 30% sucrose PBS at 4°C. Tissues were frozen at −35°C in O.C.T. Compound (Sakura Finetek U.S.A., Inc, Torrance, USA), sectioned transversely at 30 µm on a Leica SM2000R sliding microtome (Leica, Dollard-des-Ormeaux, QC, Canada), collected in PBS, and then processed as free-floating sections.

Sections were washed in PBS and pretreated with 0.3% $H_2O_2$ for 1 h. The sections were blocked in 0.3% Triton X-100 supplemented with 3% normal goat serum (Iba1 staining) or 10% fetal bovine serum (GFAP staining) in PBS for 1 h at room temperature. They were then rinsed twice with PBS and incubated at 4°C overnight with the primary antibody Iba1 or GFAP (rabbit anti-Iba1, 1:2500, Wako, Osaka, Japan; chicken anti-GFAP, 1:15000, Chemicon, Millipore) diluted with 0.3% triton and 1% normal goat serum or 3% fetal bovine serum, respectively. Sections were then rinsed with PBS and incubated for 1 h in biotin-conjugated goat anti-rabbit or goat anti-chicken IgG (Iba1: goat anti-rabbit 1:200, Vector Labs, Burlingame, CA; GFAP: goat anti-chicken 1:200, Vector Labs, Burlingame, CA) diluted with 0.3% triton and 1% normal goat serum or 3% fetal bovine serum, respectively, and finally processed for 1 h in Elite ABC solution (Vector Laboratories; prepared according to the manufacturer's instructions). The product of immune reaction was revealed using 3,3′-diaminobenzidine (DAB, Sigma-Aldrich) as a chromogen and 0.015% $H_2O_2$. The sections were mounted on SuperFost Plus slides (VWR, Ontario, Canada), dehydrated in graded ethanol, defatted in xylene, and mounted with Permount (Fisher Scientific, Montreal, QC, Canada). To minimize variability, immunohistochemical staining of the sections from each animal was performed at the same time. The specificity of each assay was determined by omitting the primary or secondary antibody.

Images were acquired on a Leica DM4000B epifluorescence microscope (Leica Microsystems, Toronto, Canada), using the same acquisition parameters (gain, exposure time). Captured images were analyzed using ImageJ software. For each animal, 10 randomly selected sections were used for Iba1 or GFAP immunostaining quantification. Region of interest consisted in laminae 1 and 2 of the dorsal horn of the spinal cord. Three to four animals per experimental conditions were analyzed. For Iba1 immunostaining analysis, images were run as 16-bit and a minimum threshold of 40 (arbitrary units) and a maximum threshold of 114 were set for each image. Particle sizes between 50 and 5000 pixels were included in the analysis. For GFAP immunostaining analysis, cells were counted manually. For both stainings, the number of particles was counted according to the region of interest.

### Chronic inflammatory pain model

Under isoflurane anesthesia (5%), 100 µL of complete Freund's Adjuvant (CFA) emulsified 1:1 with saline 0.9% and containing 4 mg/mL of dessicated *Mycobacterium butyricum* was injected in the plantar surface of the left hindpaw of Sprague-Dawley rats. Sham animals received an intraplantar injection of 100 µL saline (0.9%). One and 25 hours after CFA administration, rats received an i.t. administration of saline, NC1 (5 µg) or CCR2-6M7 (5 µg) DsiRNA. As the four duplexes performed similarly in the acute experiments, only one of them was used in a chronic inflammatory pain paradigm. Five days post-CFA, mechanical hypersensitivity was assessed with the up-down method of Dixon (1980). Testing was initiated with a 2.0 g von Frey hair. In the absence of a paw withdrawal response, a stronger stimulus was used. In the event of paw withdrawal, a weaker stimulus was applied. Four additional stimulations with weaker/stronger hair were performed following the initial response. The cut-off was set at the 15.0 g hair. The 50% g threshold was calculated using the method described in Chaplan et al.[45] with a δ value of 0.197.

### Statistical analysis

Data are presented as mean ± standard error of mean (SEM). For quantitative real-time PCR experiments, one-way ANOVA followed by Dunnett's post hoc test was used to compare gene silencing efficiency of anti-CCR2 DsiRNAs with mismatch control. Von Frey data were compared using nonparametric Kruskal-Wallis tests. Glial cell activation differences were compared using a one-way ANOVA followed by Dunnett's post hoc test. Statistical differences are presented using a threshold of significance of $p < 0.05$, $p < 0.01$, or

$p < 0.001$. Calculations were performed with GraphPad Prism 6.

## Results

### *In vitro validation of DsiRNAs targeting rCCR2 mRNA*

Ten different DsiRNAs specific for the rat CCR2 gene (NM_021866) were synthesized and characterized in vitro for their ability to decrease rCCR2 mRNA levels in a HEK293 cell line stably expressing rCCR2. A mismatch DsiRNA, consisting of a random nucleotide sequence unable to recognize any rat gene, and the transfection reagent alone were used as controls. Cells were treated for 24 h with increasing concentrations of anti-rCCR2 DsiRNAs (0.1, 1, and 10 nM), while only the highest concentration (10 nM) was used for the mismatch control. Their ability to reduce rCCR2 gene mRNA expression was determined by reverse transcription-quantitative real-time polymerase chain reaction (qPCR), with the mismatch DsiRNA used to set the remaining mRNA level to 100% (Figure 1). Two DsiRNA, CCR2-5 and CCR2-6, were highly effective in inhibiting CCR2 expression at 1 and 10 nM and were still able to reduce CCR2 mRNA levels by 60% at the lower concentration tested (0.1 nM).

For optimization, methyl groups were added to the two most potent DsiRNA candidates, CCR2-5 and CCR2-6 in order to improve in vivo duplex stability and to reduce potential immunostimulatory activity.[46–48] Both CCR2-5 and CCR2-6 were modified by adding 7 (M7 pattern) or 10 (Evader pattern) 2′-O-methyl (2′-OMe) modified RNA bases on the antisense strand. All modified candidates showed strong RNAi activity, exhibiting >85% knockdown at 10 nM (Figure 2; $^{***}p < 0.001$). Also note that the M7 modification pattern significantly improved the potency of the CCR2-6 DsiRNA to knockdown rCCR2CCR2 mRNA, compared to the Evader methylation pattern ($^{\#\#\#}p < 0.001$). However, since all methylated candidates maintained good efficiency in vitro, they have all been tested in vivo for their ability to reverse CCL2-induced pain hypersensitivity.

### *Cellular uptake of fluorescently labeled DsiRNAs by CNS tissues*

Before behavioral testing, we first assessed the ability of the cell-penetrating peptide reagent Transductin to deliver DsiRNAs in CNS tissues.[44] Tranductin-associated Texas-Red-labeled mismatch control DsiRNAs (5 µg) were administered twice in a 24 h interval by i.t. injection between the L5 and L6 vertebrae. The cellular uptake of DsiRNAs was evaluated by confocal microscopy in lumbar DRG, 24 h following the last injection (Figure 3).

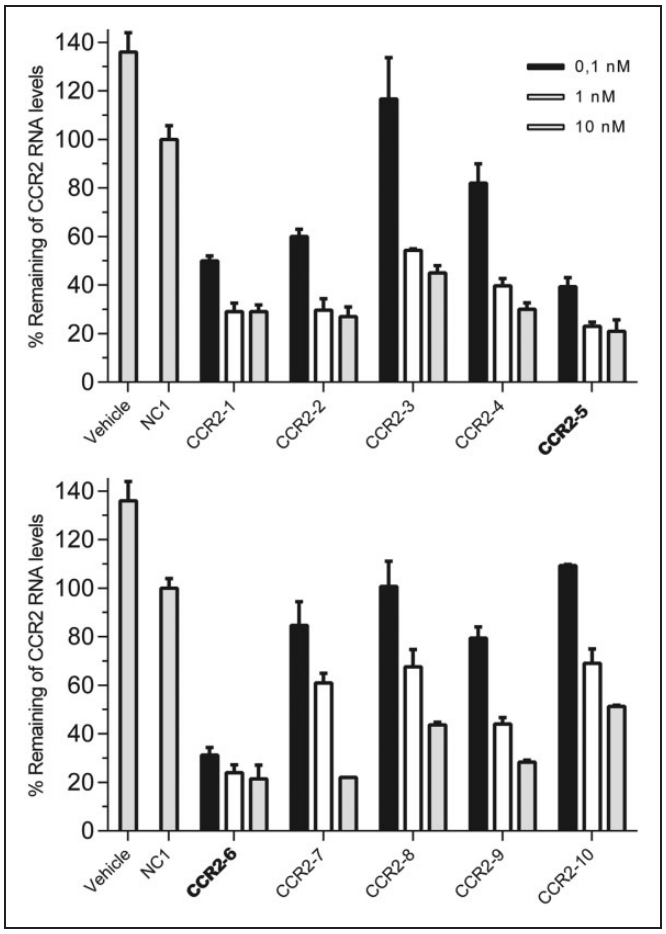


**Figure 1.** In vitro validation of anti-rCCR2 DsiRNAs. Ten 27-mer DsiRNA duplexes against rCCR2 were transfected in HEK293 cells stably expressing the rCCR2 receptor. Cells were treated with increasing doses of DsiRNAs complexed with the delivery reagent RNAiMAX, 24 h before RNA extraction. rCCR2 mRNA quantification was then assessed by quantitative real-time PCR. As a control, cells were also treated with RNAiMAX alone (vehicle group). Knockdown levels of CCR2 were normalized to levels of internal control RLPO and HPRT and normalized to the negative mismatch control = 100%. Duplexes 5 and 6 were considered as the most potent and were used for further optimization. Bars represent mean ± SEM, $n = 3$.

Confocal images revealed intense red fluorescence staining throughout the cytoplasm of small-, medium-, and large-sized primary sensory neurons, indicating that the cellular uptake of DsiRNAs by DRG neurons may affect the afferent nociceptive transmission (Figure 3(a) and (b)). Only a few sporadically scattered labeled neurons were observed at the corresponding L5–L6 lumbar dorsal horn (Figure 3(c)).

### *Attenuation of rCCR2 gene expression by DsiRNAs*

Since DsiRNAs were able to efficiently reach and penetrate sensory neurons, we next examined their ability

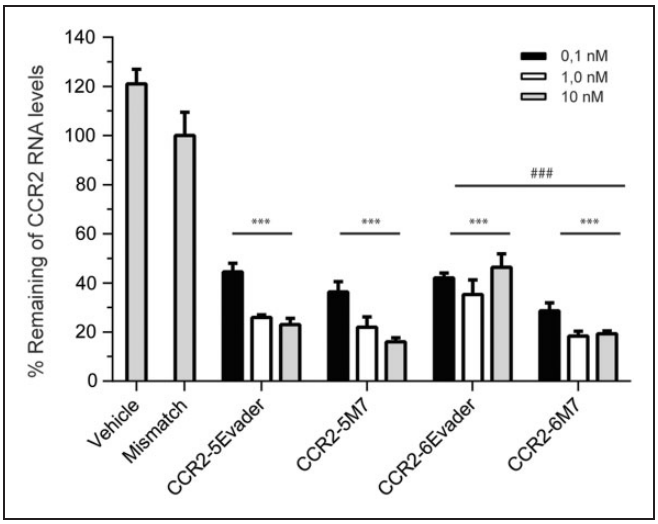


**Figure 2.** Optimization of rCCR2 DsiRNAs. Each DsiRNA sequence was tested with two different 2′-OMe patterns (M7 and Evader) on the antisense strand. HEK293 cells stably expressing rCCR2 were treated with increasing doses of DsiRNAs complexed with the delivery reagent RNAiMAX, 24 h before RNA extraction. As a control, cells were also treated with RNAiMAX alone (vehicle group). mRNA knockdown activity of rCCR2 27-mer DsiRNAs was determined by qPCR. Bars represent mean ± SEM, $n = 3$. $^{***}p < 0.001$ as compared to the mismatch control. $^{\#\#\#}p < 0.001$ refers to comparison between the Evader and M7 methylation patterns for a same dose of DsiRNA.

to silence CCR2 expression in vivo. For quantitative real-time PCR analysis, tissues were harvested 24 h after the last injection of DsiRNAs. Consistent with in vitro results, all four candidates were efficient in inhibiting rCCR2 mRNA expression (Figure 4(a)). Indeed, the use of anti-CCR2-5Evader and anti-CCR2-6Evader resulted in a 55% decrease in CCR2 transcripts in lumbar DRGs, compared to the mismatch control group ($^{**}p < 0.01$). Likewise, a significant down-regulation of CCR2 mRNA was observed following i.t. delivery of CCR2-5M7 or CCR2-6M7, reaching 71% ($^{**}p < 0.01$) and 51% ($^{*}p < 0.05$) decrease, respectively. Interestingly, all DsiRNAs developed against the rCCR2CCR2 receptor were also effective in reducing CCL2 mRNA expression (Figure 4(b)), thus suggesting that CCR2 receptor manipulation also alters the expression pattern of its ligand CCL2.

## *Anti-rCCR2 DsiRNAs prevent CCL2-induced allodynia in rat*

We previously demonstrated that spinal delivery of exogenous CCL2 induces the development of mechanical allodynia within 30 min, which persists for four consecutive days following administration.[11] Based on the ability of CCL2 to induce mechanical hypersensitivity, we decided to use this acute pain model to determine the effectiveness of anti-CCR2 DsiRNAs to prevent the onset of tactile allodynia. Toward this end, rats received two i.t. injection (5 μg) of CCR2-5Evader, CCR2-6Evader, CCR2-5M7, CCR2-6M7, or mismatch control complexed with the transfection agent Transductin (75 μg) within 24-h interval prior to a bolus i.t. injection of exogenous CCL2 (1 μg). Mechanical hypersensitivity was measured each day starting at 4 h and up to seven days after CCL2 injection (Figure 5).

Naïve rats receiving exogenous CCL2 exhibited nociceptive behaviors as early as 4 h after i.t. administration. The behavioral signs of mechanical hypersensitivity characterized by a reduction in paw withdrawal threshold were sustained for seven consecutive days (Figure 5(a) and (b)). All four candidates, designed to target different sequences distributed across the rCCR2 mRNA or carrying distinct methylation patterns, were found to be effective at blocking CCL2-induced mechanical sensitivity (Figure 5(c) and (d), $p \leqslant 0.05$). Importantly, the CCL2 nociceptive action was prevented over the seven days observation period. No statistical difference was observed between Evader and M7 2′-OMe modified duplexes. We also controlled for OTEs with the administration of mismatch control DsiRNAs, 48 h and 24 h prior to CCL2 injection. Mismatch DsiRNA did not alter CCL2-induced allodynia throughout the seven days testing period, thus suggesting that the antiallodynic effect observed results from selective down-regulation of rCCR2 mRNA. Altogether, these results demonstrate that CCR2 represents an appropriate molecular target for pain control.

## *Glial cell reactivity following CCL2 and anti-rCCR2 DsiRNAs treatment*

Accumulating evidence indicates that spinal delivery of CCL2 in naïve rats leads to spinal glial activation and enhances nociceptive transmission.[11,12,49,50] In an attempt to understand the potential role of CCR2 in triggering glial cell activation which is also known to participate in central sensitization and pain hypersensitivity, we investigated the effect of anti-rCCR2 DsiRNA treatments on glial cell reactivity in the superficial layers of the spinal dorsal horn.

Twenty-four hours following CCL2 i.t. administration, Iba1-positive microglial cells exhibited enlarged cell bodies, characteristic of their active state, as opposed to the ramified resting state observed in saline-treated rats. This increase in cell body area was not accompanied by changes in microglial cell density (Figure 6; Table 4). In the same experimental paradigm, the number and polygonal morphology of GFAP-positive astrocytes remained unchanged (Figure 6; Table 4). Also note that no differences were observed between saline/saline and saline/mismatch (NC1) groups,

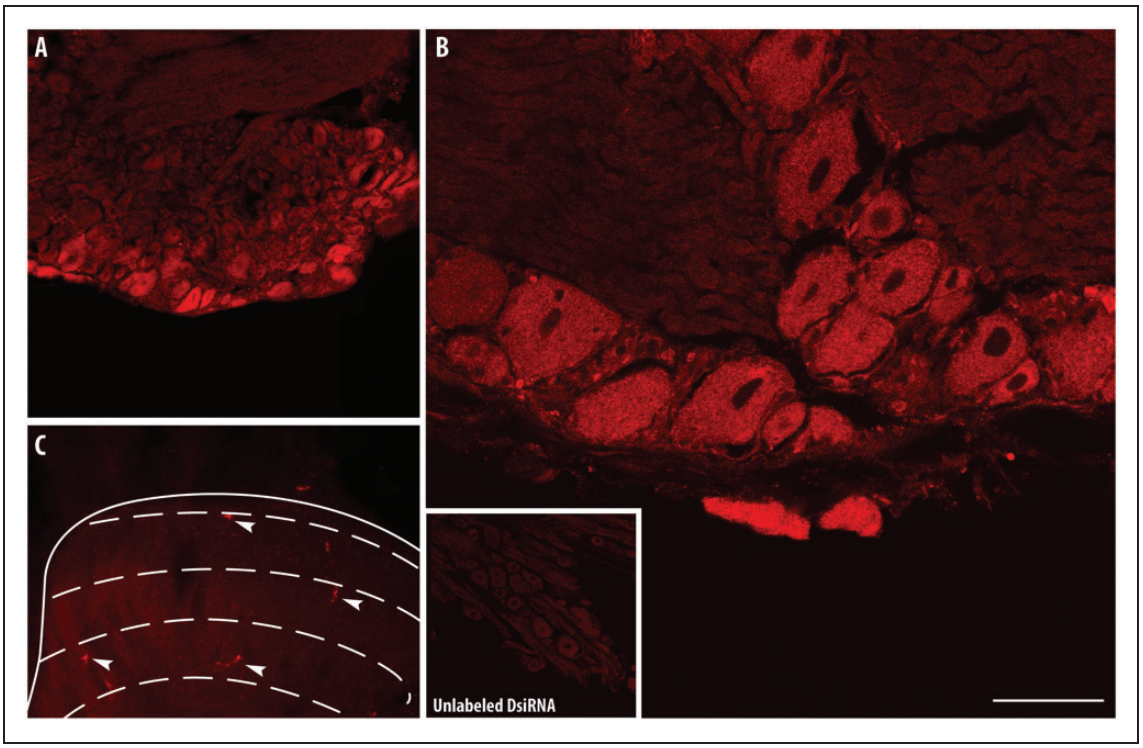


**Figure 3.** Penetration of Texas-Red-labeled DsiRNAs in lumbar dorsal root ganglion and spinal cord neurons. Distribution of fluorescence in different subpopulations of DRG neurons following intrathecal delivery of a control DsiRNAs tagged with Texas-red (5 μg administered twice with a 24-h interval; $n = 3$) at low and high magnification (a, b). A NC1 unlabeled DsiRNAs was used as control (b, inset). Only a few sporadically scattered labeled neurons were evident in the superficial dorsal horn (c, arrowheads). Effective uptake of Texas-red-tagged DsiRNAs was captured by laser-scanning confocal microscopy. Scale bars = 120 μm in (a); 40 μM in (b); 320 μM in (c); 200 μM in inset.

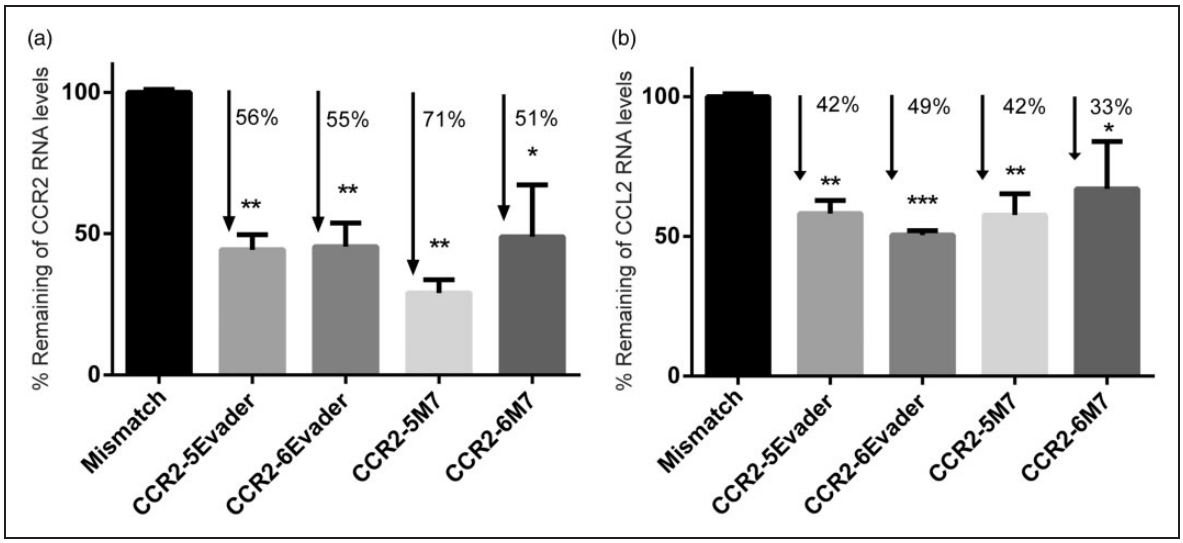


**Figure 4.** Changes in rCCR2 and rCCL2 gene expression in dorsal root ganglia following in vivo DsiRNA delivery. Down-regulation of CCR2 (a) and CCL2 (b) mRNA levels in DRGs was measured by quantitative real-time PCR 24 h after a two-day pretreatment with two DsiRNA (CCR2-5 and CCR2-6), carrying distinct 2′-OMe patterns (M7 and Evader) on the antisense strand. qPCR values were normalized against internal control genes HPRT and Odc. Each column corresponds to the mean ± SEM of six biological samples done in triplicate. The knockdown efficiency is expressed in percentage and compared to CCL2-injected rats treated with mismatch control DsiRNA (one-way ANOVA followed by Dunnett's post hoc test; $^{*}p < 0.05$, $^{**}p < 0.01$, $^{***}p < 0.001$ compared to mismatch control).

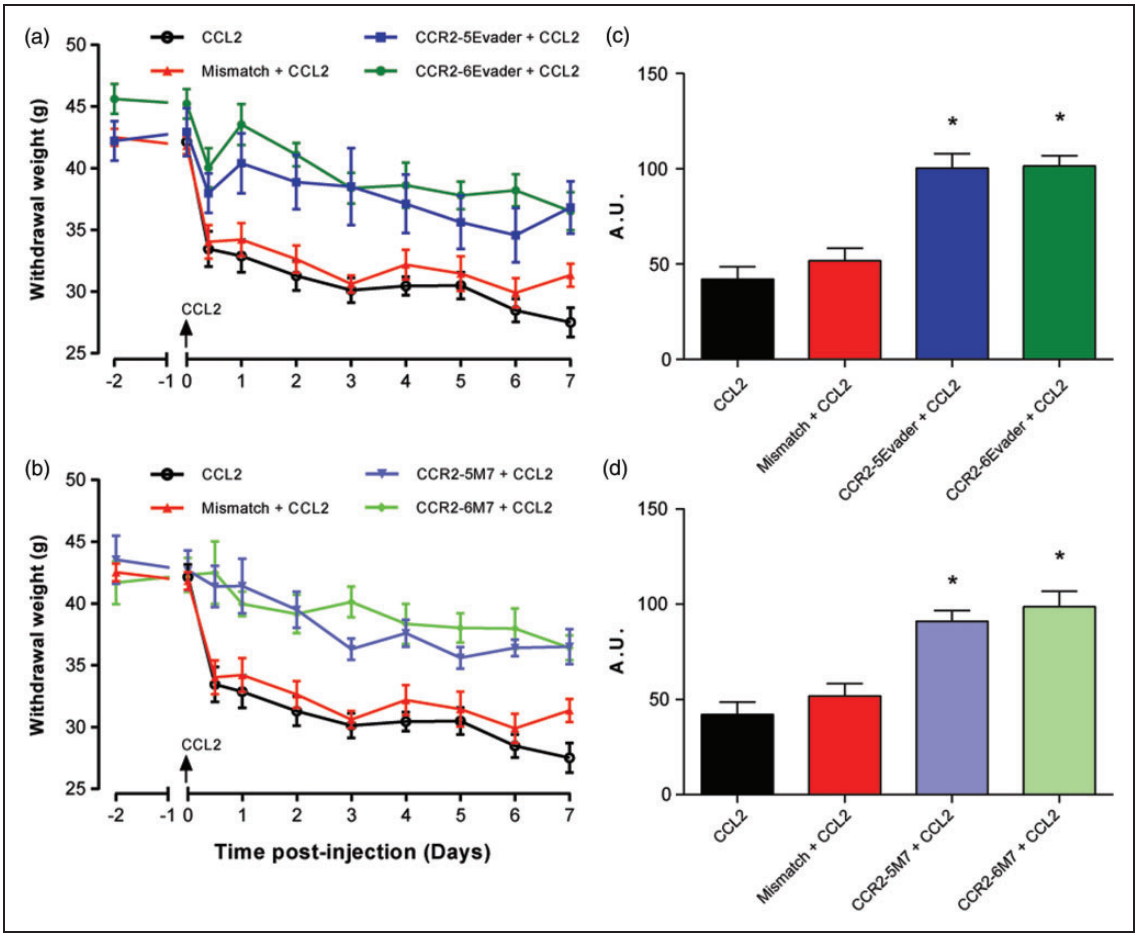


**Figure 5.** Reduction of CCL2-induced mechanical allodynia by CCR2 DsiRNA treatment. The paw withdrawal threshold was assessed using a von Frey automatic plantar aesthesiometer 24 h after the last of two daily i.t. injections of Evader (a) or M7 (b) methylated DsiRNAs. The area under the curve (AUC) was calculated in arbitrary units throughout the whole testing period ((c) and (d)). All DsiRNA targeting CCR2 significantly reduced CCL2-induced tactile allodynia. The CCL2 group received two i.t. administration of saline instead of DsiRNA. Data are expressed as mean ± SEM ($n = 6$ for CCL2 and each duplex group. $n = 20$ for mismatch controls). *$p < 0.05$ as compared to CCL2-treated rats.

indicating that i.t. exposure to DsiRNAs did not induce glia activation.

Following spinal delivery of rCCR2 DsiRNAs prior to CCL2 injection, microglial cells appeared to return to a resting state, as characterized by a significant decrease in their cell body area. Furthermore, as opposed to mismatch-treated rats, rats receiving rCCR2 DsiRNAs exhibited a spinal astrocyte cell population in a slightly hypertrophic state. Finally, CCR2-DsiRNA treatment did not induce any changes in the density of microglial or astrocyte cells.

### *Anti-rCCR2 DsiRNAs reduce chronic inflammatory pain*

Accumulating evidence suggests that blocking the CCL2-CCR2 signaling axis can counteract the hypernociceptive symptoms resulting from a chronic pain state.[17,18] We thus evaluated whether DsiRNAs against rCCR2CCR2 were able to attenuate the hypernociceptive responses in the CFA-induced inflammatory chronic pain. One and 25 hours following intraplantar administration of CFA, rats received two i.t. injection of saline, NC1 (5 µg) or CCR2-6M7 (5 µg). Treatment with CCR2-6M7 almost completely reversed the mechanical hypersensitivity observed five days following CFA (Figure 7; $p < 0.01$), indicating that this RNAi-based gene therapy represents a targeted approach for treating inflammatory pain.

## Discussion

Recent studies have highlighted the role of the CCL2/CCR2 axis in the development and maintenance of nociceptive processing at the spinal level.[12,19,20,51,52] Thus, CCR2 has become a potential therapeutic target for

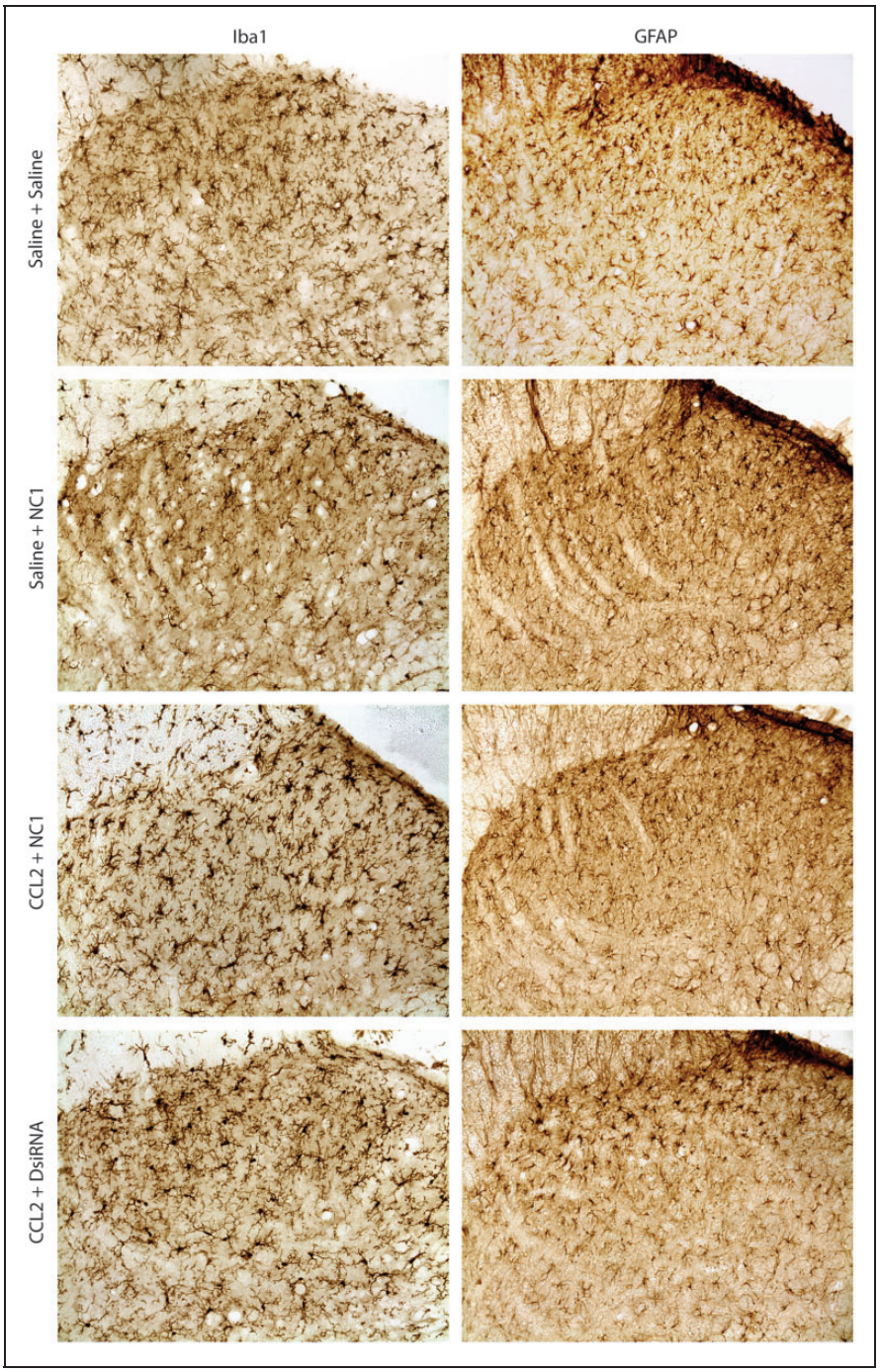


**Figure 6.** Modulation of CCL2-induced glial cell activation by anti-rCCR2 DsiRNAs. Immunohistochemical labeling of spinal microglia cells and astrocytes identified by Iba1 and GFAP stainings, respectively. Rats received two injections of anti-rCCR2 DsiRNA (CCR2-6M7) or mismatch control (NC1M7) and a single CCL2 or saline injection. Data are expressed as mean ± SEM ($n = 3$ animals per condition).

pain management and significant progress has been made in the design and synthesis of novel CCR2 antagonists.[53,54] Nevertheless, development of potent and selective CCR2 antagonists is facing several challenges, including selectivity against other chemokine receptors and ion channels, and poor activity at the rodent receptor.[55] Indeed, a characteristic of the chemokine receptor family is the promiscuity of chemokines for multiple receptors. For instance, CCR2, CCR5, and CCR1 share significant sequence homology and it is therefore not surprising to observe cross-reactivity of CCR2 antagonists with CCR5 or some level of activity at CCR1. Likewise, some CCR2 antagonists exhibit off-target activities by acting at the cardiac hERG/IKr

**Table 4.** Glial cell quantification and morphology analysis.

| | Saline + Saline | Saline + NC1 | CCL2 + NC1 | CCL2 + DsiRNA |
|---|---|---|---|---|
| Microglial cell body area ($\mu m^2$) | $108 \pm 4$ | $105 \pm 3$ | $139 \pm 8^{***}$ | $118 \pm 3^{\#}$ |
| Microglial cell density (number/$mm^2$) | $321 \pm 16$ | $343 \pm 15$ | $367 \pm 22$ | $337 \pm 11$ |
| Astrocyte cell body area ($\mu m^2$) | $13.8 \pm 1.2$ | $12.9 \pm 1.2$ | $12.5 \pm 0.7$ | $14.7 \pm 0.6^{*}$ |
| Astrocyte density (number/$mm^2$) | $477 \pm 26$ | $457 \pm 16$ | $469 \pm 11$ | $458 \pm 27$ |

Differences in glial cell activation were determined using a one-way ANOVA followed by Dunnett's post hoc test. $^{*}p < 0.05$ or $^{***}p < 0.001$ as compared to saline + NC1. $^{\#}p < 0.05$ as compared to CCL2-treated rats. NC1 refers to the mismatch control DsiRNA.

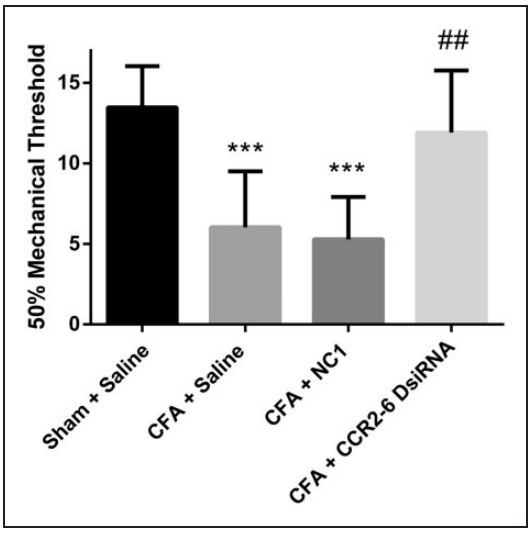


**Figure 7.** DsiRNAs targeting CCR2 reduce mechanical hypersensitivity in a chronic inflammatory pain model. The 50% mechanical threshold was assessed five days after intraplantar administration of either CFA or saline. One and 25 hours following CFA injection, rats were treated i.t. with saline, NC1 (5 μg), or CCR2-6M7 (5 μg) DsiRNA. Data are expressed as mean ± SEM ($n = 6$ animals). $^{***}p < 0.001$ compared to sham animals. $^{\#\#}p < 0.01$ compared to CFA animals treated with mismatch control (NC1M7).

potassium channel, thus disqualifying them from any consideration for advancement into the clinic. Species selectivity is also an important issue in the development of small molecule CCR2 antagonists. Many compounds designed as inhibitors of human CCR2 have very low potency at rodent receptors, which has led to serious challenges in predictability and interpretation of preclinical experimental data to human.[55,56] Not surprisingly therefore, all of these limitations may explain in part the failures of CCR2 antagonists in clinical trials.[57] Other explanations may also account for these clinical failures, including the high redundancy in the chemokine receptor-ligand pairing and the fact that some chemokine receptors do not have a single binding site for their ligands.[56,58] Acting as allosteric modulators, small molecule antagonists may indeed bind to multiple sites on the receptor and evoke distinct patterns of intracellular signaling.[59] This is further reinforced by the fact that chemokine receptors exhibit biased signaling to different ligands, and that some ligands behave as agonists to one receptor and antagonists to another.[60,61] While chemokine receptor antagonists still represent an extremely fruitful avenue for optimizing treatment outcomes in various chronic illnesses,[57] the complexities of the chemokine system require the implementation of novel approaches distinct from conventional pharmacological interventions. To overcome hurdles associated with chemokine antagonists, we used here a RNAi-based therapeutic technology to target the CCL2/CCR2 chemokine network within the spinal cord.

In the present study, we first screened a series of Dicer-substrate-siRNAs designed to target different sequences distributed across the rCCR2 mRNA for their in vitro mRNA knockdown activity. While not predicting in vivo efficacy, this first step is crucial since siRNA potency frequently varies among different target sites within a same gene.[62] This process allowed us to identity two potent duplexes (CCR2-5 and CCR2-6), exhibiting strong RNAi activity even at very low concentration (>60% knockdown at 0.1 nM). However, when used in an in vivo setting, a number of drawbacks needs to be overcome, including nuclease stability, strand loading, activation of the innate immune system, efficient delivery of DsiRNAs to the target cell population, and OTEs.[31] Among them, one of the most reported side effects identified with the first generations of siRNAs was an immune response upon stimulation of the nucleic acid-sensing TLRs and protein kinase R (PKR).[33,34,63] Today, strategies exist to enable synthetic siRNA to evade detection by the innate immune system through design and chemical modifications. One of these strategies used to avoid induction of type 1 interferon response to dsRNA molecules is the addition of methyl groups in position two (2′-OMe) of the ribose backbone.[64] This chemical modification mimics the natural methylation process occurring in mammalian rRNA and tRNA maturation.[65] It has been reported that 2′-OMe decreases protein kinase R and TLR7 activation through competitive inhibition.[66] Furthermore, 2′-O-methylations increase siRNAs duplex stability against nuclease degradation which greatly contributes

to enhance in vivo half-life and minimize OTEs.[42,65,67,68] This reduction in immunogenicity is, however, sometimes accompanied by a lack of efficacy due to allosteric obstruction of the methyl groups causing interference with the interaction of Dicer and Ago2. In addition to 2′OMe modification, other 2′modifications, such as 2′F and locked nucleic acids (LNA), also help to reduce the risk of triggering immune response.[31] CCR2-5 and CCR2-6 DsiRNAs were thus methylated through two different patterns without interfering with their ability to down-regulate rCCR2 mRNA in vitro, although the Evader methylation pattern reduced the CCR2-6 potency compared to the M7 pattern. Both modifications were also able to reduce CCR2 expression in vivo, although once again the M7 methylation seems to be more potent than the Evader for CCR2-5.

Lack of safe and efficient delivery of siRNA to target tissues or organs also constitutes a serious obstacle to using this technology for a host of diseases.[29,32,69,70] Because of their high molecular weight (~14 kDa) and highly polyanionic nature, naked DsiRNAs, like siRNAs, do not freely diffuse across cell membrane. Indeed, naked RNA usually gives poor silencing rates at low doses and become toxic at high doses.[36,71] Therefore, a delivery system is required to facilitate DsiRNAs access to their intracellular site of action.[72] The most commonly used nonviral delivery method involves cationic lipid reagents or liposome formulations.[73] These reagents were found to be effective for many cell lines but showed limited efficacy with primary cells or nonadherent cell types. Likewise, low concentrations of transfection reagents are required to limit cellular toxicity or immune responses in certain cell types.[74,75] The use of cell-penetrating peptides is another nonviral siRNA delivery approach that has gained a lot of interest in recent years. This approach mediates cellular uptake of macromolecules into a variety of hard-to-transfect cells such as neurons with low cytotoxicity and high efficiency in vivo.[47,76,77] These peptides consist of multiple Peptide Transduction Domains connected to a Double-Stranded RNA Binding Domain (PTD-DRBD). When complexed with RNA duplexes, they bind to cell surface glycosaminoglycans and are up-taken through the process of macropinocytosis. In order to evaluate the capacity of the peptide-based transfection reagent Transductin to induce DsiRNA cellular uptake in vivo, we intrathecally injected Texas-Red-labeled DsiRNAs. Confocal microscopy imaging revealed strong fluorescence staining in DRG cells indicating that DsiRNAs were able to reach their site of action. There, they were also able to significantly reduce the levels of rCCR2 mRNA. The data for all duplexes showed that 24 h after the last injection of DsiRNAs, CCR2 mRNA levels were reduced by more than 50% compared to mismatch DsiRNA-treated rats. These results are consistent with previous studies showing that DsiRNAs exhibited in vivo knockdown activities ranging from 40 to 80%.[42,78–81] Interestingly, we also found that knockdown of CCR2 impacts on CCL2 expression, since a reduction in the levels of CCL2 mRNA was observed following treatment with each CCR2 DsiRNAs tested, independently of the methylation pattern and sequence targeted. These results thus support the existence of cross-regulation mechanisms between CCR2 and CCL2. Accordingly, activation of CCR2 leads to an increase in p38 MAPK, which in turn regulates the production of CCL2.[82,83]

As opposed to the efficient uptake of fluorescence-tagged DsiRNAs by sensory neurons, only a few sporadically scattered labeled neurons were however detected in lumbar dorsal horn. This almost absence of fluorescence staining may be explained by the considerable distance required to deliver the fluorescence-tagged DsiRNA from the site of injection (where the spinal nerves forms the *Cauda equina*) to the corresponding lumbar spinal cord segments. Consequently, this may indicate that the in vivo effects observed following i.t. delivery of anti-CCR2 DsiRNAs are probably driven by primary sensory neurons. Any observations made in the spinal cord would be therefore secondary to CCR2 knockdown in DRG tissues. Since the exogenous CCL2 is not lasting seven days but probably initiates a cascade of molecular events leading to the persistent pain state, we can thus speculate that the down-regulation of CCR2 by DsiRNA treatment occurring at the DRG level impedes these early signal transduction events. This hypothesis is supported by previous studies demonstrating the central role of the CCL2/CCR2 signaling in sensory neuron excitability.[11,84–88]

One of the other shortcomings of siRNA approaches are sequence-specific OTEs that are caused by partial hybridization of siRNAs with unintended gene and disruption of endogenous microRNA pathway.[89–91] This often occurs following siRNA dose-response curves and may be prevented by using the minimum effective dose.[92] Within the cytoplasm, 27-mer DsiRNAs mimic the substrate of the Dicer enzyme due to their length and enter into the endogenous RNAi pathway one step earlier than siRNAs, thus favoring a greater incorporation into the RISC complex.[38,40] Indeed, DsiRNAs are as much as 10 times more potent than standard siRNAs with longer duration of gene silencing effects which leads to the use of significantly lower concentrations to reach the same efficacy.[37,41,42] Furthermore, the inclusion of a 3′ overhang on the antisense strand confers more homogeneity in Dicer products compared to blunt 27-mers while also reducing OTEs.[38] To ensure that the physiological observations made were the results of a specific RNAi effect and not related to some unsuspected OTEs, the in vivo experiments were performed with two DsiRNAs, targeting different sequences within the CCR2

mRNA and carrying distinct 2′-OMe patterns. Our data demonstrate that all four DsiRNA candidates significantly reduced or even completely blocked CCL2-induced tactile allodynia, compared to mismatch DsiRNA-treated rats. Along with similar reductions of CCR2 mRNA levels, both sequences and methylation patterns were similarly effective in inhibiting acute pain development for the whole seven days of the testing period. Sequence-dependent OTEs are therefore unlikely to be responsible for the CCL2-reversed pronociceptive activity.

As the CCL2-CCR2 signaling axis has been pointed as a key contributor in the development of painful sensations associated with chronic inflammatory and neuropathic pain conditions,[8,19,21,93] we were also expecting these analgesic actions to be reflected in a pathophysiological model of chronic inflammatory pain. Accordingly, spinal delivery of DsiRNAs targeting CCR2 in the early time points following the initiation of a long-lasting and painful inflammatory challenge completely blocked the mechanical hypersensitivity five days after the first injection. Interestingly, pharmacological intervention to prevent CCL2-induced mechanical hypersensitivity was reported to be efficient for only two days, after which treated animals reverted back to their hypersensitive state.[11] This suggests that knocking down CCR2 with DsiRNA allows for a more complete and sustained inactivation than the use of some small molecule CCR2 antagonists, even though they only reduce rCCR2 mRNA by 50%. Although the precise mechanisms behind such a disparity remain to be elucidated, it hints toward some biased signaling of CCL2 that is not systematically prevented by CCR2 antagonists.[59,61] Another explanation may rely on the fact that the anti-CCR2 DsiRNAs selectively penetrate into DRG tissues and not into lumbar dorsal horn.

In recent years, chemokines have been described to play an important role in neuron-glia communication.[22,94] There is indeed a great line of evidence suggesting that chemokines behave as neuromodulators/neurotransmitters within the CNS and that not only glial cells but also neurons can express chemokines and chemokine receptors.[3] Despite the fact that the precise cellular localization of CCR2 and CCL2 still remains controversial,[5,22,95] the involvement of the CCL2/CCR2 pathway in the dynamic communication between neurons and neighboring glial cells as well as the contribution of CCL2/CCR2 for the development of central sensitization and pain hypersensitivity are not debated. Our results demonstrated that 24 h following i.t. CCL2 administration, microglial cells but not astrocytes displayed an activated phenotype. These results are consistent with previous studies which have reported microglia activation following spinal CCL2 delivery.[19] Besides, the lack of changes in microglial cell density may be explained by the early time-point (24 h) used to analyze microglial cell reactivity following exogenous CCL2 administration. Indeed, most of the literature reports that microglial cell proliferation only occurs three days following injury in neuropathic pain models.[96–98] Cell proliferation may therefore be an event downstream to microglial cell hypertrophy in the cascade of events leading to a hyperactive phenotype. We also found that in addition to reverse the allodynic state induced by spinal CCL2, anti-rCCR2 DsiRNAs prevented CCL2-induced microglial cell activation. These data are in agreement with previous findings demonstrating impaired nociceptive responses and the lack of microglial cell activation in CCR2 KO mice.[20,50,99] In the same experimental paradigm, astroglial cells were found in a slightly hypertrophic state in anti-rCCR2 DsiRNA-treated animals as opposed to rats treated with mismatch control, which cannot be explained by the increased sensitivity of astrocytes over microglia to lipid-carried siRNA.[100] These morphological changes in glia cells resulting specifically from the knockdown of CCR2 in DRG tissues further reinforce the key role played by chemokines in neuron-glia communication.

## Conclusion

Altogether, we demonstrated here that Dicer-substrate-siRNAs targeting CCR2 delivered spinally were able to reach the cell body of sensory neurons, reduce CCR2 expression and microglial activation, and finally induce a persistent inhibition of the nociceptive behaviors induced by acute injection of exogenous CCL2 or following induction of a chronic inflammatory pain state. These results validate CCR2 as a target for pain management and demonstrate the promise of RNAi-based gene therapy approaches for selectively inhibiting complex targets, such as chemokines and their potential for treating pain.

### Authors' contributions

VBL carried out the rCCR2 mRNA quantification, the in vivo behavioral tests and drafted the manuscript. EM performed the characterization of glial cells and drafted the manuscript. MAD performed the CFA experiments and participated to draft the manuscript. PT carried out the cellular uptake of DsiRNAs and helped in the mRNA quantification of rCCR2. JML participated in the design and coordination of the study. AJ and SR designed the DsiRNAs and carried out the in vitro validation of the DsiRNAs. MB, NB, and PS conceived, designed, and coordinated the study. VBL and EM contributed equally to this work.

### Declaration of Conflicting Interests

The author(s) declared the following potential conflicts of interest with respect to the research, authorship, and/or publication of this article: MAB, SDR, and AMJ are employed by

Integrated DNA Technologies Inc. (IDT), which offers oligonucleotides for sale similar to some of the compounds described in the manuscript. However, IDT is not a publicly traded company and these authors do not own any shares or hold equity in IDT.

## Funding

The author(s) disclosed receipt of the following financial support for the research, authorship, and/or publication of this article: This work is supported by a grant from the Canadian Institutes of Health Research (CIHR) awarded to PS. PS is a recipient of the Canada Research Chair in Neurophysiology of Chronic Pain; Director of the Quebec Pain Research Network and the Sherbrooke's Neuroscience Centre; and Codirector of the Sherbrooke's Institut de Pharmacologie. VBL and MAD hold a CIHR scholarship award. PT is the recipient of a doctoral scholarship from the National Sciences and Engineering Research Council of Canada (NSERC). EM holds a scholarship from the Fonds de Recherche du Québec en Santé (FRQS) and the Réseau de Recherche en Santé Buccodentaire et osseuse (RSBO).

## References

1. Viola A and Luster AD. Chemokines and their receptors: drug targets in immunity and inflammation. *Annu Rev Pharmacol Toxicol* 2008; 48: 171–197.
2. Baggiolini M. Chemokines and leukocyte traffic. *Nature* 1998; 392: 565–568.
3. Rostène W, Dansereau M-AA, Godefroy D, et al. Neurochemokines: a menage a trois providing new insights on the functions of chemokines in the central nervous system. *J Neurochem* 2011; 118: 680–694.
4. Miller RJ, Jung H, Bhangoo SK, et al. Cytokine and chemokine regulation of sensory neuron function. *Handb Exp Pharmacol* 2009; 194: 417–449.
5. Gao YJ and Ji RR. Chemokines, neuronal-glial interactions, and central processing of neuropathic pain. *Pharmacol Ther* 2010; 126: 56–68.
6. White FA and Miller RJ. Insights into the regulation of chemokine receptors by molecular signaling pathways: functional roles in neuropathic pain. *Brain Behav Immun* 2010; 24: 859–865.
7. Gosselin RD, Dansereau MA, Pohl M, et al. Chemokine network in the nervous system: a new target for pain relief. *Curr Med Chem* 2008; 15: 2866–2875.
8. Abbadie C. Chemokines, chemokine receptors and pain. *Trends Immunol* 2005; 26: 529–534.
9. White FA, Jung H and Miller RJ. Chemokines and the pathophysiology of neuropathic pain. *Proc Natl Acad Sci USA* 2007; 104: 20151–20158.
10. Tanaka T, Minami M, Nakagawa T, et al. Enhanced production of monocyte chemoattractant protein-1 in the dorsal root ganglia in a rat model of neuropathic pain: possible involvement in the development of neuropathic pain. *Neurosci Res* 2004; 48: 463–469.
11. Dansereau MA, Gosselin RD, Pohl M, et al. Spinal CCL2 pronociceptive action is no longer effective in CCR2 receptor antagonist-treated rats. *J Neurochem* 2008; 106: 757–769.
12. Thacker MA, Clark AK, Bishop T, et al. CCL2 is a key mediator of microglia activation in neuropathic pain states. *Eur J Pain* 2009; 13: 263–272.
13. Bhangoo SK, Ripsch MS, Buchanan DJ, et al. Increased chemokine signaling in a model of HIV1-associated peripheral neuropathy. *Mol Pain* 2009; 5: 48.
14. Serrano A, Pare M, McIntosh F, et al. Blocking spinal CCR2 with AZ889 reversed hyperalgesia in a model of neuropathic pain. *Mol Pain* 2010; 6: 90.
15. Van Steenwinckel J, Reaux-Le Goazigo A, Pommier B, et al. CCL2 released from neuronal synaptic vesicles in the spinal cord is a major mediator of local inflammation and pain after peripheral nerve injury. *J Neurosci* 2011; 31: 5865–5875.
16. Zhang ZJ, Dong YL, Lu Y, et al. Chemokine CCL2 and its receptor CCR2 in the medullary dorsal horn are involved in trigeminal neuropathic pain. *J Neuroinflammation* 2012; 9: 136.
17. Llorián-Salvador M, Pevida M, González-Rodríguez S, et al. Analgesic effects evoked by a CCR2 antagonist or an anti-CCL2 antibody in inflamed mice. *Fundam Clin Pharmacol* 2016; 30: 235–247.
18. Okamoto M, Suzuki T and Watanabe N. Modulation of inflammatory pain in response to a CCR2/CCR5 antagonist in rodent model. *Journal Pharmacol Pharmacother* 2013; 4: 208–210.
19. Menetski J, Mistry S, Lu M, et al. Mice overexpressing chemokine ligand 2 (CCL2) in astrocytes display enhanced nociceptive responses. *Neuroscience* 2007; 149: 706–714.
20. Abbadie C, Lindia JA, Cumiskey AM, et al. Impaired neuropathic pain responses in mice lacking the chemokine receptor CCR2. *Proc Natl Acad Sci USA* 2003; 100: 7947–7952.
21. Miller RE, Tran PB, Das R, et al. CCR2 chemokine receptor signaling mediates pain in experimental osteoarthritis. *Proc Natl Acad Sci USA* 2012; 109: 20602–20607.
22. Old EA and Malcangio M. Chemokine mediated neuron-glia communication and aberrant signalling in neuropathic pain states. *Curr Opin Pharmacol* 2012; 12: 67–73.
23. Colobran R, Pujol-Borrell R, Armengol MP, et al. The chemokine network. I. How the genomic organization of chemokines contains clues for deciphering their functional complexity. *Clin Exp Immunol* 2007; 148: 208–217.
24. Nedjai B, Li H, Stroke IL, et al. Small-molecule chemokine mimetics suggest a molecular basis for the observation that CXCL10 and CXCL11 are allosteric ligands of CXCR3. *Br J Pharmacol* 2012; 166: 912–923.
25. Berchiche YA, Gravel S, Pelletier ME, et al. Different effects of the different natural CC chemokine receptor 2b ligands on beta-arrestin recruitment, Galphai signaling, and receptor internalization. *Mol Pharmacol* 2011; 79: 488–498.
26. Kenakin T. New concepts in drug discovery: collateral efficacy and permissive antagonism. *Nat Rev Drug Discov* 2005; 4: 919–927.
27. Horuk R. Chemokine receptor antagonists: overcoming developmental hurdles. *Nat Rev Drug Discov* 2009; 8: 23–33.
28. Davidson BL and McCray PB Jr. Current prospects for RNA interference-based therapies. *Nat Rev Genet* 2011; 12: 329–340.

29. Borna H, Imani S, Iman M, et al. Therapeutic face of RNAi: in vivo challenges. *Expert Opin Biol Ther* 2015; 15: 269–285.
30. Burnett JC, Rossi JJ and Tiemann K. Current progress of siRNA/shRNA therapeutics in clinical trials. *Biotechnol J* 2011; 6: 1130–1146.
31. Rettig GR and Behlke MA. Progress toward in vivo use of siRNAs-II. *Mol Ther* 2012; 20: 483–512.
32. Wittrup A and Lieberman J. Knocking down disease: a progress report on siRNA therapeutics. *Nat Rev Genet* 2015; 16: 543–552.
33. Robbins M, Judge A and MacLachlan I. siRNA and innate immunity. *Oligonucleotides* 2009; 19: 89–102.
34. Whitehead KA, Dahlman JE, Langer RS, et al. Silencing or stimulation? siRNA delivery and the immune system. *Ann Rev Chem Biomol Eng* 2011; 2: 77–96.
35. Tan PH, Gao YJ, Berta T, et al. Short small-interfering RNAs produce interferon-α-mediated analgesia. *Br J Anaesth* 2012; 108: 662–669.
36. Sarret P, Doré-Savard L, Tétreault P, et al., eds. *Application of dicer-substrate siRNA in pain research*. Berlin: RNA Technologies Springer, 2010.
37. Kim DH, Behlke MA, Rose SD, et al. Synthetic dsRNA Dicer substrates enhance RNAi potency and efficacy. *Nat Biotechnol* 2005; 23: 222–226.
38. Rose SD, Kim DH, Amarzguioui M, et al. Functional polarity is introduced by Dicer processing of short substrate RNAs. *Nucleic Acids Res* 2005; 33: 4140–4156.
39. Snead NM, Wu X, Li A, et al. Molecular basis for improved gene silencing by Dicer substrate interfering RNA compared with other siRNA variants. *Nucleic Acids Res* 2013; 41: 6209–6221.
40. Hefner E, Clark K, Whitman C, et al. Increased potency and longevity of gene silencing using validated Dicer substrates. *J Biomol Tech* 2008; 19: 231–237.
41. Kubo T, Zhelev Z, Ohba H, et al. Modified 27-nt dsRNAs with dramatically enhanced stability in serum and long-term RNAi activity. *Oligonucleotides* 2007; 17: 445–464.
42. Dudek H, Wong DH, Arvan R, et al. Knockdown of β-catenin with dicer-substrate siRNAs reduces liver tumor burden in vivo. *Mol Ther* 2014; 22: 92–101.
43. Dore-Savard L, Roussy G, Dansereau MA, et al. Central delivery of Dicer-substrate siRNA: a direct application for pain research. *Mol Ther* 2008; 16: 1331–1339.
44. Eguchi A, Meade BR, Chang YC, et al. Efficient siRNA delivery into primary cells by a peptide transduction domain-dsRNA binding domain fusion protein. *Nat Biotechnol* 2009; 27: 567–571.
45. Chaplan SR, Bach FW, Pogrel JW, et al. Quantitative assessment of tactile allodynia in the rat paw. *J Neurosci Methods* 1994; 53: 55–63.
46. Collingwood MA, Rose SD, Huang L, et al. Chemical modification patterns compatible with high potency dicer-substrate small interfering RNAs. *Oligonucleotides* 2008; 18: 187–200.
47. Jackson AL and Linsley PS. Recognizing and avoiding siRNA off-target effects for target identification and therapeutic application. *Nat Rev Drug Discov* 2010; 9: 57–67.
48. Morrissey DV, Lockridge JA, Shaw L, et al. Potent and persistent in vivo anti-HBV activity of chemically modified siRNAs. *Nat Biotechnol* 2005; 23: 1002–1007.
49. Huang CY, Chen YL, Li AH, et al. Minocycline, a microglial inhibitor, blocks spinal CCL2-induced heat hyperalgesia and augmentation of glutamatergic transmission in substantia gelatinosa neurons. *J Neuroinflammation* 2014; 11: 7.
50. Zhang J, Shi XQ, Echeverry S, et al. Expression of CCR2 in both resident and bone marrow-derived microglia plays a critical role in neuropathic pain. *J Neurosci* 2007; 27: 12396–12406.
51. Zhu X, Cao S, Zhu M-DD, et al. Contribution of chemokine CCL2/CCR2 signaling in the dorsal root ganglion and spinal cord to the maintenance of neuropathic pain in a rat model of lumbar disc herniation. *J Pain* 2014; 15: 516–526.
52. LaCroix-Fralish ML, Austin JS, Zheng FY, et al. Patterns of pain: meta-analysis of microarray studies of pain. *Pain* 2011; 152: 1888–1898.
53. Pease JE and Horuk R. Chemokine receptor antagonists: part 2. *Exp Opin Ther Pat* 2009; 19: 199–221.
54. Pease JE and Horuk R. Chemokine receptor antagonists: part 1. *Exp Opin Ther Pat* 2009; 19: 39–58.
55. Struthers M and Pasternak A. CCR2 antagonists. *Curr Top Med Chem* 2010; 10: 1278–1298.
56. Proudfoot AE, Power CA and Schwarz MK. Anti-chemokine small molecule drugs: a promising future? *Expert Opin Investig Drugs* 2010; 19: 345–355.
57. Solari R, Pease JE and Begg M. Chemokine receptors as therapeutic targets: why aren't there more drugs? *Eur J Pharmacol* 2015; 746: 363–367.
58. Zweemer AJ, Bunnik J, Veenhuizen M, et al. Discovery and mapping of an intracellular antagonist binding site at the chemokine receptor CCR2. *Mol Pharmacol* 2014; 86: 358–368.
59. Ajram L, Begg M, Slack R, et al. Internalization of the chemokine receptor CCR4 can be evoked by orthosteric and allosteric receptor antagonists. *Eur J Pharmacol* 2014; 729: 75–85.
60. Kenakin T and Christopoulos A. Signalling bias in new drug discovery: detection, quantification and therapeutic impact. *Nat Rev Drug Discov* 2013; 12: 205–216.
61. Zweemer AJ, Toraskar J, Heitman LH, et al. Bias in chemokine receptor signalling. *Trends Immunol* 2014; 35: 243–252.
62. Filhol O, Ciais D, Lajaunie C, et al. DSIR: assessing the design of highly potent siRNA by testing a set of cancer-relevant target genes. *PloS one* 2012; 7: e48057.
63. Kurreck J. RNA interference: from basic research to therapeutic applications. *Angew Chem Int Ed Engl* 2009; 48: 1378–1398.
64. Judge AD, Bola G, Lee AC and et al. Design of noninflammatory synthetic siRNA mediating potent gene silencing in vivo. *Mol Ther* 2006; 13: 494–505.
65. Behlke MA. Chemical modification of siRNAs for in vivo use. *Oligonucleotides* 2008; 18: 305–319.
66. Robbins M, Judge A, Liang L, et al. 2′-O-methyl-modified RNAs act as TLR7 antagonists. *Mol Ther* 2007; 15: 1663–1669.

67. Choung S, Kim YJ, Kim S, et al. Chemical modification of siRNAs to improve serum stability without loss of efficacy. *Biochem Biophys Res Commun* 2006; 342: 919–927.
68. Gaglione M and Messere A. Recent progress in chemically modified siRNAs. *Mini Rev Med Chem* 2010; 10: 578–595.
69. Prabha S, Vyas R, Gupta N, et al. RNA interference technology with emphasis on delivery vehicles-prospects and limitations. *Artif Cells, Nanomed Biotechnol* 2015; July: 1–9.
70. Sioud M. Strategies for siRNA navigation to desired cells. *Methods Mol Biol* 2015; 1218: 201–216.
71. Sarret P, Doré-Savard L, Tétreault P, et al. (eds). *Using RNA interference to down-regulate GPCRs. G-protein-coupled receptor technology*. New York: Springer-Verlag, 2011.
72. Whitehead KA, Langer R and Anderson DG. Knocking down barriers: advances in siRNA delivery. *Nat Rev Drug Discov* 2009; 8: 129–138.
73. Lv H, Zhang S, Wang B, et al. Toxicity of cationic lipids and cationic polymers in gene delivery. *J Control Release* 2006; 114: 100–109.
74. Breunig M, Lungwitz U, Liebl R, et al. Breaking up the correlation between efficacy and toxicity for nonviral gene delivery. *Proc Natl Acad Sci USA* 2007; 104: 14454–14459.
75. Lonez C, Vandenbranden M and Ruysschaert J-MM. Cationic lipids activate intracellular signaling pathways. *Adv Drug Deliv Rev* 2012; 64: 1749–1758.
76. Gump JM and Dowdy SF. TAT transduction: the molecular mechanism and therapeutic prospects. *Trends Mol Med* 2007; 13: 443–448.
77. Eguchi A and Dowdy SF. siRNA delivery using peptide transduction domains. *Trends Pharmacol Sci* 2009; 30: 341–345.
78. Darniot M, Schildgen V, Schildgen O, et al. RNA interference in vitro and in vivo using DsiRNA targeting the nucleocapsid N mRNA of human metapneumovirus. *Antivir Res* 2012; 93: 364–373.
79. Lundberg P, Yang HJ, Jung SJ, et al. Protection against TNFalpha-dependent liver toxicity by intraperitoneal liposome delivered DsiRNA targeting TNFalpha in vivo. *J Control Release* 2012; 160: 194–199.
80. Pichu S, Krishnamoorthy S, Zhang B, et al. Dicer-substrate siRNA inhibits tumor necrosis factor alpha secretion in Kupffer cells in vitro: in vivo targeting of Kupffer cells by siRNA-liposomes. *Pharmacol Res* 2012; 65: 48–55.
81. Zhou J, Neff CP, Liu X, et al. Systemic administration of combinatorial dsiRNAs via nanoparticles efficiently suppresses HIV-1 infection in humanized mice. *Mol Ther* 2011; 19: 2228–2238.
82. Kuang Y, Wu Y, Jiang H, et al. Selective G protein coupling by C-C chemokine receptors. *J Biol Chem* 1996; 271: 3975–3978.
83. Sugimoto T, Morioka N, Zhang FF, et al. Clock gene Per1 regulates the production of CCL2 and interleukin-6 through p38, JNK1 and NF-κB activation in spinal astrocytes. *Mol Cell Neurosci* 2014; 59: 37–46.
84. Belkouch M, Dansereau M-AA, Réaux-Le Goazigo A, et al. The chemokine CCL2 increases Nav1.8 sodium channel activity in primary sensory neurons through a Gβγ-dependent mechanism. *J Neurosci* 2011; 31: 18381–18390.
85. Jung H and Miller RJ. Activation of the nuclear factor of activated T-cells (NFAT) mediates upregulation of CCR2 chemokine receptors in dorsal root ganglion (DRG) neurons: a possible mechanism for activity-dependent transcription in DRG neurons in association with neuropathic pain. *Mol Cell Neurosci* 2008; 37: 170–177.
86. Qin X, Wan Y and Wang X. CCL2 and CXCL1 trigger calcitonin gene-related peptide release by exciting primary nociceptive neurons. *J Neurosci Res* 2005; 82: 51–62.
87. White FA, Bhangoo SK and Miller RJ. Chemokines: integrators of pain and inflammation. *Nat Rev Drug Discov* 2005; 4: 834–844.
88. Zhang H, Boyette-Davis JA, Kosturakis AK, et al. Induction of monocyte chemoattractant protein-1 (MCP-1) and its receptor CCR2 in primary sensory neurons contributes to paclitaxel-induced peripheral neuropathy. *J Pain* 2013; 14: 1031–1044.
89. Grimm D, Streetz KL, Jopling CL, et al. Fatality in mice due to oversaturation of cellular microRNA/short hairpin RNA pathways. *Nature* 2006; 441: 537–541.
90. Jackson AL, Bartz SR, Schelter J, et al. Expression profiling reveals off-target gene regulation by RNAi. *Nat Biotechnol* 2003; 21: 635–637.
91. John M, Constien R, Akinc A, et al. Effective RNAi-mediated gene silencing without interruption of the endogenous microRNA pathway. *Nature* 2007; 449: 745–747.
92. Caffrey DR, Zhao J, Song Z, et al. siRNA off-target effects can be reduced at concentrations that match their individual potency. *PLoS One* 2011; 6: e21503.
93. Belkouch M, Dansereau M-AA, Tétreault P, et al. Functional up-regulation of Nav1.8 sodium channel in Aβ afferent fibers subjected to chronic peripheral inflammation. *J Neuroinflammation* 2014; 11: 45.
94. Sheridan GK and Murphy KJ. Neuron-glia crosstalk in health and disease: fractalkine and CX3CR1 take centre stage. *Open Biol* 2013; 3: 130181.
95. Biber K and Boddeke E. Neuronal CC chemokines: the distinct roles of CCL21 and CCL2 in neuropathic pain. *Front Cell Neurosci* 2014; 8: 210.
96. Suter MR, Wen Y-RR, Decosterd I, et al. Do glial cells control pain? *Neuron Glia Bio* 2007; 3: 255–268.
97. Echeverry S, Shi XQ and Zhang J. Characterization of cell proliferation in rat spinal cord following peripheral nerve injury and the relationship with neuropathic pain. *Pain* 2008; 135: 37–47.
98. Zhang J and De Koninck Y. Spatial and temporal relationship between monocyte chemoattractant protein-1 expression and spinal glial activation following peripheral nerve injury. *J Neurochem* 2006; 97: 772–783.
99. El Khoury J, Toft M, Hickman SE, et al. Ccr2 deficiency impairs microglial accumulation and accelerates progression of Alzheimer-like disease. *Nat Med* 2007; 13: 432–438.
100. Gorina R, Santalucia T, Petegnief V, et al. Astrocytes are very sensitive to develop innate immune responses to lipid-carried short interfering RNA. *Glia* 2008; 57: 93–107.